

Brefeldin A rapidly disrupts plasma membrane polarity by blocking polar sorting in common endosomes of MDCK cells

Exing Wang¹, Janice G. Pennington¹, James R. Goldenring², Walter Hunziker³ and Kenneth W. Dunn^{1,*}

¹Department of Medicine, Division of Nephrology, Indiana University Medical Center, Indianapolis, IN 46202, USA

²Departments of Medicine, Surgery and Cellular Biology and Anatomy, Institute of Molecular Medicine and Genetics, Medical College of Georgia and the Augusta VA Medical Center, Augusta, GA 30912, USA

³Institute of Molecular and Cell Biology, 30 Medical Drive, Singapore 117609

*Author for correspondence (e-mail: kwduinn@iupui.edu)

Accepted 28 May 2001

Journal of Cell Science 114, 3309-3321 (2001) © The Company of Biologists Ltd

SUMMARY

Recent studies showing thorough intermixing of apical and basolateral endosomes have demonstrated that endocytic sorting is critical to maintaining the plasma membrane polarity of epithelial cells. Our studies of living, polarized cells show that disrupting endocytosis with brefeldin-A rapidly destroys the polarity of transferrin receptors in MDCK cells while having no effect on tight junctions. Brefeldin-A treatment induces tubulation of endosomes, but the sequential compartments and transport steps of the transcytotic pathway remain intact. Transferrin is sorted from LDL, but is then missorted from common endosomes to the apical recycling endosome, as identified by its nearly neutral pH, and association with GFP chimeras of Rabs 11a and 25. From the apical recycling endosome, transferrin is then directed to the apical plasma membrane.

These data are consistent with a model in which polarized sorting of basolateral membrane proteins occurs via a brefeldin-A-sensitive process of segregation into basolateral recycling vesicles. Although disruption of polar sorting correlates with dissociation of γ -adaptin from endosomes, γ -adaptin does not appear to be specifically involved in sorting into recycling vesicles, as we find it associated with the transcytotic pathway, and particularly to the post-sorting transcytotic apical recycling endosome.

Movies available on-line

Key words: Endocytosis, Polarity, Transferrin, Epithelium, MDCK cell

INTRODUCTION

The barrier and transport functions of an epithelium depend upon the polarized distribution of proteins and lipids on its luminal and basal aspects. This polarity is established through a process of sorting of newly synthesized proteins in the trans-Golgi network and in endosomes, and through selective retention of proteins via interactions with the cytoskeleton. Plasma membrane polarity is maintained despite continuous endocytic turnover. Whereas endosomes derived from the apical and basolateral plasma membrane domains were once considered distinct from one another (Bomsel et al., 1989; Parton et al., 1989), more recent studies indicate that the two are continuously and thoroughly intermixed (Apodaca et al., 1994; Futter et al., 1998; Odorizzi et al., 1996; Wang et al., 2000). Thus, efficient endocytic sorting is also critical to maintaining plasma membrane polarity.

Recent studies have implicated AP-1 adaptor complex molecules in polar sorting in epithelial cells. Expression of a novel μ 1b subunit in epithelial cells restored the polarity of the low density lipoprotein (LDL) receptor and the transferrin receptor (TfR) in LLC-Pk1 cells with defective polarity (Folsch et al., 1999). Another AP-1 protein, γ -adaptin, has been associated with basolateral recycling vesicles containing TfR

(Futter et al., 1998). Based upon the observation that treatment of cells with Brefeldin A (BFA) dissociated γ -adaptin from endosomes and also increased aberrant delivery of TfR to the apical membrane of MDCK cells (Wan et al., 1992; Matter et al., 1993; Futter et al., 1998), Futter et al. proposed that polar sorting in endosomes occurs by a process in which γ -adaptin-associated endosomal buds mediate sorting of basolateral membrane proteins into basolateral recycling vesicles.

According to this model, BFA blocks polar sorting by impairing sequestration of basolateral proteins into recycling vesicles. However, the effects of BFA on endocytosis are clearly not limited to basolateral recycling. In fact, earlier studies demonstrated that BFA selectively inhibits transcytosis of IgA with little effect on basolateral recycling (Hunziker et al., 1991). Prydz et al. (Prydz et al., 1992) report that BFA selectively increases apical endocytosis, and stimulates basolateral to apical transcytosis of both membrane and fluid markers. BFA has also been found to inhibit efflux of apically transcytosing pIgR from the apical recycling endosome (ARE) (Barroso and Sztul, 1994). Observations that BFA induces ectopic transport of a variety of internalized proteins (Hunziker et al., 1991; Matter et al., 1993) suggest that, rather than impairing transport, BFA blocks polar sorting.

However, in light of these diverse effects, it is difficult to

interpret the effects of BFA on specific intracellular transport steps from its effects on whole cell fluxes. In fact, it could also be concluded that each of these observations reflects non-specific consequences of a gross disruption of endosome structure induced by BFA. In particular, impaired sorting might be expected as a non-specific consequence of the fusion of endocytic compartments (Lippincott-Schwartz et al., 1991; Wood et al., 1991; Wagner et al., 1994).

Here we use microscopy of living cells to assess how defined endocytic compartments are disrupted by BFA, and combine microscopic and biochemical assays to address the question of whether BFA-sensitive factors are required for polarized sorting in endosomes. We have previously demonstrated that polar sorting occurs in common endosomes from which transferrin (Tf) is directly recycled and IgA is transcytosed to the ARE (Brown et al., 2000). In the studies presented here we find that although BFA tubulates endosomes, the sequential compartments of the transcytotic pathway remain intact in BFA-treated cells, with distinct sorting endosomes, common endosomes and AREs. In the context of this intact pathway, we determined that BFA induces missorting of Tf onto the transcytotic pathway from common endosomes to the ARE, and then to the apical plasma membrane.

These studies support the hypothesis that basolateral sorting occurs via a BFA-sensitive segregation of basolateral membrane proteins into recycling vesicles (Futter et al., 1998). While, as previously observed, BFA treatment dissociated γ -adaptin from endosome membranes, we find γ -adaptin associated more closely with transcytotic IgA than with recycling Tf, in fact associated with the post-sorting transcytotic ARE. These observations indicate that γ -adaptin does not play a specific role in basolateral recycling, but rather participates in both transcytosis and basolateral recycling. The effects of BFA on recycling and transcytosis may be explained by the association of γ -adaptin with both pathways, or alternatively, may reflect different BFA-sensitive coats involved in basolateral recycling and transcytosis.

MATERIALS AND METHODS

Cells

Fluorescence studies were conducted using PTR cells, MDCK strain II cells transfected with both the human TfR and the rabbit pIgR, previously described (Brown et al., 2000; Wang et al., 2000). The biochemical sorting assays were conducted in MDCK cells transfected with both rabbit pIgR and human TfR. Cells expressing pIgR (Hunziker and Peters, 1998) were transfected with the pCB6 plasmid containing the human TfR. We verified that the polarity and the kinetics of internalization and recycling were similar to those of the endogenous TfR.

GFP chimeras on the amino termini of rabbit Rab11a and Rab25 were generated from full-length cDNAs amplified by PCR using Pfu polymerase (Stratagene) and cloned in-frame into the pEGFP-C2 vector (Clontech). Sequences were verified by complete sequencing of an amplified insert (Medical College of Georgia Molecular Biology Core Facility). Stable lines expressing GFP-Rab25 were generated by transfection of pWE MDCK cells expressing the rabbit pIgR (Breitfeld et al., 1989) and selection in G-418. GFP-Rab11a was transiently expressed in PTR cells by transfecting cells prior to seeding onto filters, where they were cultured for 3 days prior to imaging.

For fluorescence experiments, PTR or pWE cells were plated at

confluence on the bottoms of collagen-coated Millipore CM filters and cultured for 4-5 days prior to experiments, as described previously (Brown et al., 2000; Wang et al., 2000). Electron microscopy and biochemical sorting studies were conducted with cells grown on polycarbonate filters (Costar Corp.).

Proteins and chemicals

Purified dimeric IgA was provided by Prof. J.-P. Vaerman (Catholic University of Louvain, Brussels, Belgium). Human Tf was obtained from Sigma, iron-loaded and purified as described (Yamashiro et al., 1984). Human LDL was obtained from Biomedical Technologies, Inc. (Stoughton, MA, USA). With the exception of Cyanine 5.18 (Cy5), which was obtained from Amersham Co. (Arlington Heights, IL, USA), all fluorescent probes were obtained from Molecular Probes. Tf conjugated to horseradish peroxidase (HRP-Tf) was obtained from Jackson Immunoresearch (West Grove, PA, USA). BFA was obtained from Epicentre Technologies (Madison, WI, USA). All other reagents were obtained from Sigma Chem Co. (St Louis, MO, USA). Fluorescent ligands were prepared as described previously (Brown et al., 2000; Wang et al., 2000).

Labeling of cells with fluorescent ligands

Cells were incubated at 37°C on a slide warmer in a humidified chamber for 15 minutes prior to addition of fluorescent ligands. All incubations were conducted in Medium 1 (150 mM NaCl, 20 mM Hepes, 1 mM CaCl₂, 5 mM KCl, 1 mM MgCl₂, 10 mM glucose pH 7.4). As described in each study, cells were labeled with 20 μ g/ml fluorescent Tf, 20 μ g/ml fluorescent LDL or 100 μ g/ml fluorescent IgA. In nearly all cases, cells were imaged alive, in the continued presence of ligands. For localization of γ -adaptin, labeled filters were rinsed briefly in PBS at 4°C, then fixed with 4% paraformaldehyde in pH 7.4 PBS at 4°C for 15 minutes.

The specificity of receptor-mediated uptake of fluorescent LDL, IgA and Tf was demonstrated by its inhibition by competition with excess unlabeled ligands. Fluorescent IgA and Tf were both found to efflux the cells with kinetics similar to those of the radiolabeled ligands. Dual labeling experiments showed the endosomal distributions of ligands conjugated to different fluorophores to be identical.

Microscopy

Microscopy was conducted using either a Bio-Rad MRC-1024 confocal attachment mounted on a Nikon Eclipse 200 inverted microscope using a Nikon 60 \times , N.A. 1.2 water immersion objective or on a Zeiss LSM-510 confocal microscope, using a Zeiss 63X, N.A. 1.2 water immersion objective. Image volumes were collected by collecting a vertical series of images, each between 0.4 and 0.6 μ m apart. Photomultiplier offsets were set such that background was slightly positive to guarantee signal linearity with fluorescence. Whenever possible signal saturation was avoided, and objects with saturated pixels were omitted from quantifications. For live cell studies, incubations were conducted in medium 1 on the microscope stage, with basolateral ligands added to the filter cup, while apical ligands are added to the well of the coverslip-bottomed dish. Temperature is maintained by a Medical Systems Corp. PDMI-2 open perfusion chamber (Greenvale, NY, USA). Fixed cells were imaged in PBS containing 2% DABCO (Sigma Co.).

Electron microscopy

Polarized cells grown on Costar transwell filters were incubated for 30 minutes with 15 μ g/ml transferrin conjugated to horseradish peroxidase (HRP-Tf) (Jackson Immunoresearch Laboratories, West Grove, PA, USA), rinsed in PBS and fixed in 2% paraformaldehyde, 2.5% glutaraldehyde in 0.1 M sodium cacodylate buffer, pH 7.4 for 30 minutes on ice.

The filters were rinsed in 0.1 M sodium cacodylate buffer, preincubated in SIGMA FAST DAB (Sigma Chem. Co., St Louis,

MO, USA) for 4 minutes in the dark, then incubated in SIGMA FAST DAB (0.7 mg/ml) with H₂O₂ (0.2 mg/ml) and nickel in 0.06 M Tris buffer, pH 7.6, for 30 minutes in the dark at room temperature. The filters were then rinsed with cacodylate buffer and post-fixed in 1% osmium tetroxide, 1% potassium ferricyanide in 0.1 M cacodylate buffer for 90 minutes. The filters were then rinsed in distilled water, en bloc-stained overnight in 0.5% aqueous uranyl acetate, dehydrated in a graded ethanol series and embedded in Spurr resin. Sections 70–80 nm thick were mounted on 200-mesh nickel grids and viewed unstained at 60 KV in a Philips CM 120 electron microscope. Digital images were captured with a Gatan 791 Multi-Scan Camera (Gatan Inc., Pleasanton, CA, USA).

Image processing

Image processing was conducted using Metamorph software (Universal Imaging, West Chester, PA, USA). To minimize photobleaching, and phototoxicity in living cells, all fields were imaged with minimal averaging (1–2 frames). To compensate, images were subsequently averaged spatially where necessary. Images shown in figures were contrast-stretched to enhance the visibility of dim structures, and specific care was taken never to enhance the contrast in such a way that dim objects were deleted from an image. Comparable images were always contrast enhanced identically. Montages were assembled and annotated using Photoshop (Adobe, Mountain View, CA, USA).

Tf uptake polarity assay

To measure the percentage of Tf internalization occurring via apical TfR, cells were incubated in 20 µg/ml Alexa568-Tf basolaterally, and 20 µg/ml Alexa488-Tf apically at 37°C. After 30 minutes, cells were rinsed and fixed and 3-D image volumes were then collected. Each image plane was then background corrected by subtracting the median intensity of a 32×32 pixel region surrounding each pixel (Maxfield and Dunn, 1990), and the planes summed together. Non-specific fluorescence was subtracted from these sums using values measured for unlabeled cells (averaging <1 gray level per image plane). The difference in the amount of fluorescence detected per mole of each probe was standardized using a factor measured from cells labeled basolaterally with an equimolar mixture of the two probes, imaged with identical settings to those used for the polarity analyses. (Alexa488-Tf=1.82 × Alexa568-Tf.). The total apical internalization was then quantified as the fraction of the sum of apical and basolateral uptake. 40 cells, chosen for sufficient basolateral uptake, without regard for apical uptake, were analyzed for both control cells, and for cells pretreated for 15 minutes and then labeled for 30 minutes in the presence of 10 µM BFA.

Fluorometric analysis of junctional permeability

To quantify monolayer permeability, 2 mg/ml fluorescein dextran (70 kDa) was added to the basolateral chamber of filters following a 15 minute preincubation in medium 1, in medium 1 with 10 µM BFA or in calcium-free PBS (containing 10 mM glucose) (3 times each). The filters were maintained in these solutions for an additional 30 minutes during which time the apical chamber of each was sampled every 5 minutes. The fluorescence of these samples were then quantified with a Cytofluor II fluorescence plate reader (PerSeptive Biosystems, Framingham, MA, USA).

Biochemical Tf-IgA sorting assay

These studies were essentially carried out as described previously (Podbilewicz and Mellman, 1990; Hunziker et al., 1991). Cells were starved and allowed to internalize 2 µg/ml of HRP-Tf (3 moles HRP per mole Tf) from the basolateral surface for 30 minutes. ¹²⁵I-dIgA (1 µg/ml), HRP-Tf (2 µg/ml) and, in some experiments, ¹²⁵I-Tfn (1 µg/ml) were bound on ice for 60 minutes, excess ligand was washed off, and cells were incubated in the absence or presence of 10 µM BFA (Sigma Chemical Co.) or 33 µM nocodazole (Sigma Chemical

Co.) for 15 minutes on ice. In all cases, the basolateral medium was supplemented with 10 µg/ml Tfn-HRP. Cells were then directly transferred to 37°C without changing medium. For preinternalization experiments, ¹²⁵I-dIgA was internalized for 5 minutes and non-internalized surface ligand was removed with acid as described (Hunziker et al., 1991).

After different periods of time cells were returned to ice, rinsed twice with PBS and then incubated in 0.5 mM 3,3'-diaminobenzidine (Sigma Chemical Co.), 0.07% H₂O₂ in PBS for 60 minutes. After washing twice with PBS, filters containing the cells were cut out of the holders and extracted in 1 ml of 1% Triton X-100, 0.2% sodium azide (to inactivate horse radish peroxidase) in PBS for 20 minutes at room temperature. Insoluble material in the detergent extracts was pelleted in a microcentrifuge (5 minutes, 14,000 g) and equal volumes of the extracts were analyzed by SDS-PAGE (8% acrylamide) and autoradiography. The radioactivity present in the detergent soluble fraction was plotted as % of the total cell associated radioactivity (sum of the radioactivity in detergent-soluble and -insoluble fractions). The radioactivity in the detergent-insoluble fraction was obtained by counting the polycarbonate filters and the pellet after centrifugation of the detergent-soluble fraction. Points were carried out in duplicate and the % values differed by less than 5%.

Similar results were obtained if the detergent-soluble fraction was normalized to total initially bound dIgA (sum of the radioactivity in apical medium, basolateral medium, detergent-soluble and -insoluble fraction); the values for the 25 minute time point were 21% (control), 10% (BFA), and 20% (nocodazole). The total initially bound radioactivity averaged 20–25,000 c.p.m. Control experiments showed that intracellular transport of HRP-Tf was similar to that of Tf: less than 1% of the cell associated HRP activity was recovered in the apical medium after 90 minutes; in the presence of BFA the transcytosed fraction of HRP activity increased to 10–15%, similar to published results for Tf (Wan et al., 1992) (not shown).

Quantifications of relative IgA and Tf fluorescence in endosomes

3-D image volumes were collected for quantitative analysis of cells labeled with Alexa488-IgA (green) and Alexa568-Tf (red). Individual images were averaged spatially, then projected (using a maximum intensity algorithm) into a single, extended-focus image. Outlines of cells were drawn by hand and the red and green pixel intensities measured for the entire selected volume. To allow the data to be pooled despite variation in the relative numbers of pIgR and TfR between cells, the green pixel intensities were multiplied by a factor calculated to give equivalent total red and green fluorescence for each cell.

Immunofluorescence localizations

For immunolocalizations of γ-adaptin, cells were labeled as indicated, then fixed as described above. Cells were then washed three times with 10 mM glycine in PBS, pH 7.4, for 10 minutes. Cells were then permeabilized in 0.025% saponin for 5 minutes and nonspecific sites were blocked in 1% BSA + 0.025% saponin + 0.05% fish skin gelatin in PBS-glycine for 5 minutes. Cells were incubated with mouse anti-γ-adaptin monoclonal antibody (clone 100/3, Sigma Chem. Co.) rinsed 3× with PBS followed by the incubation with the TxR-sheep-anti-mouse antibody (Jackson ImmunoResearch) for 1 hour at room temperature and then with TxR-donkey-anti-sheep (Jackson ImmunoResearch) at room temperature for 1 more hour.

Cross-correlation analysis

Cross correlation image analysis was conducted as described previously (van Steensel et al., 1996; Brown et al., 2000). 3-D image volumes of red and green fluorescence were collected sequentially, to guarantee no bleed-through of fluorescence from one fluorophore into the detector channel of the other. 3-D regions of the cytoplasm of

individual cells were then selected for analysis by outlining each focal plane by hand and then thresholding a low-pass filtered image, which eliminated nuclei from analysis. Images were then background corrected (Maxfield and Dunn, 1990). For each pair of images the entire 3-D volume of a single cell was compared with that of a companion volume, and a Pearson's correlation coefficient (r_p) calculated as described previously. Although cells were selected for analysis such that the overall levels of IgA or Tf fluorescence were similar, Fig. 10A shows that the correlation coefficients are independent of the levels of IgA or Tf fluorescence. Cells were selected for analysis without regard for the relative patterns of the two probes being compared. Comparisons of two colors of Tf were conducted using circular regions of interest, in order to avoid spurious effects of region mismatch when the two regions were compared after one partner volume was rotated 180°.

RESULTS

BFA rapidly disrupts plasma membrane polarity of TfR

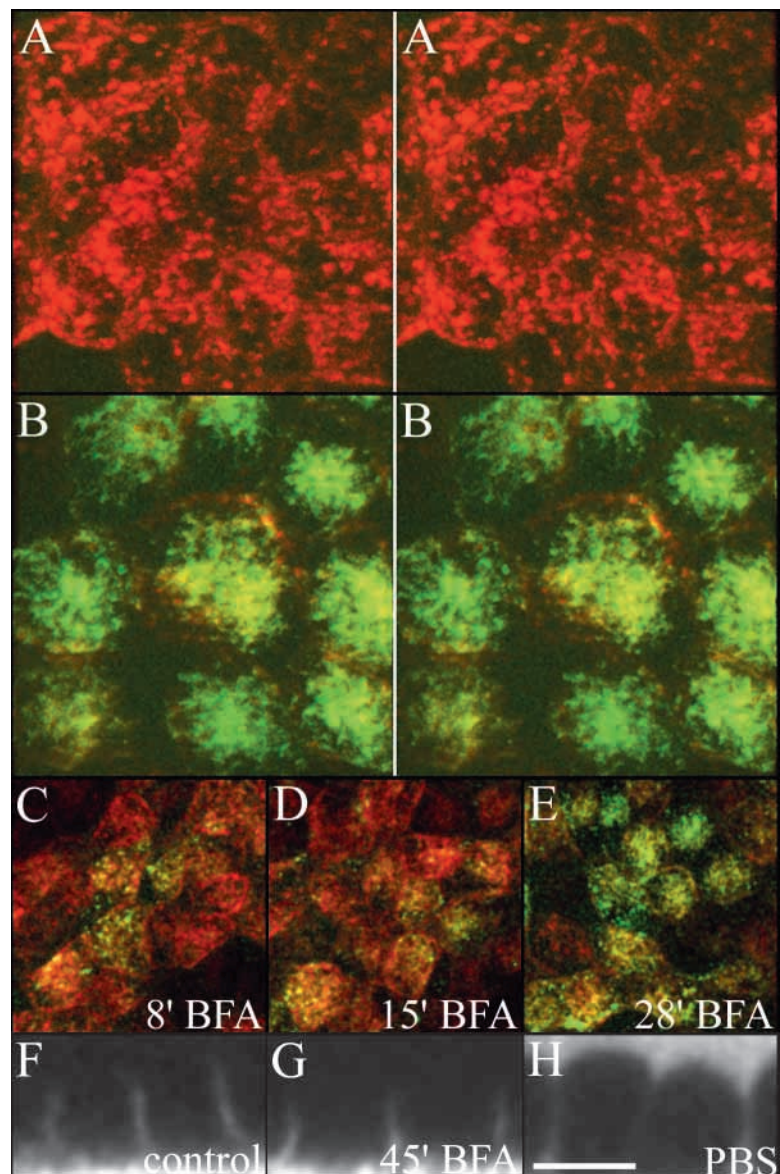
The polarized distribution of TfR to the basolateral membrane of PTR cells is apparent in image volumes of cells showing strong basolateral and minimal apical uptake of Tf. The stereopair shown in Fig. 1A shows robust uptake of basolateral Alexa568-Tf (red) by a field of living, polarized PTR cells, with no internalization of apical Alexa488-Tf (green). However, cells pretreated for 15 minutes with 10 μ M BFA (2.8 μ g/ml) prior to incubation with Tf show very pronounced uptake of apical Alexa488-Tf and a concomitant decrease in internalization of basolateral Alexa568-Tf (Fig. 1B). These 3-D images also emphasize how BFA tubulates endosomes. (Note that

Fig. 1. BFA induces apical redistribution of TfR. 3-D stereopair images of living, polarized PTR cells imaged in the presence of apical Alexa488-Tf and basolateral Alexa568-Tf after 30 minutes of uptake, following 15 minutes of pretreatment in medium lacking (A) or containing (B) 10 μ M BFA, show that BFA significantly increases apical Tf uptake. (Note that these and all subsequent 3-D stereopair images are also presented as rotating animations at <http://renal.nephrology.iupui.edu/wangetal2>). Note that the background fluorescence in these and subsequent images of living cells results from the presence of fluorescent ligands in the medium. (C-E) The speed with which BFA induces apical redistribution of TfR is shown in extended focus projected volumes of living cells preincubated with apical Alexa488-Tf and basolateral Alexa568-Tf for 20 minutes, and then in probes plus BFA for the indicated times. (F-H) Uptake of Tf from the apical chamber does not result from leakage of dye across disrupted tight junctions. (F) Vertical cross section of an image volume collected of control cells incubated with basolateral 70 kDa fluorescein dextran for 20 minutes show that the dye is limited to the basolateral medium. (G) The tight junction barrier is likewise intact in cells pretreated with 10 μ M BFA, then in dextran and BFA for another 30 minutes. (H) The junction is breached in cells pre-incubated in PBS lacking Ca^{2+} for 30 minutes, then incubated with dextran in PBS for 20 minutes, resulting in leakage of dextran into the apical space. Scale bar, 10 μ m for all panels except C-E (20 μ m).

these and all subsequent 3-dimensional stereopair images are also presented as rotating animations at <http://renal.nephrology.iupui.edu/wangetal2>).

Quantitative analysis from a comparable experiment showed that whereas apical uptake accounted for only 3.9% ($\pm 3.7\%$, $n=40$) of total Tf internalization in control cells, BFA increased apical uptake to 38.5% ($\pm 11.5\%$, $n=40$) of total cellular uptake (see Materials and Methods). Although this assay measures a composite of the number of receptors and the rates of endocytosis from each plasma membrane domain, the increased internalization of Tf from the apical membrane of BFA-treated cells primarily reflects redistribution of TfR to the apical plasma membrane. First, BFA induced a nearly proportional decline in basolateral uptake. Second, previous studies detected a two- to threefold increase in non-specific apical endocytosis in BFA-treated cells (Prydz et al., 1992), a small fraction of the increase observed here.

The speed with which TfR polarity is lost is shown in images of living cells shown in Fig. 1C-E. In this experiment



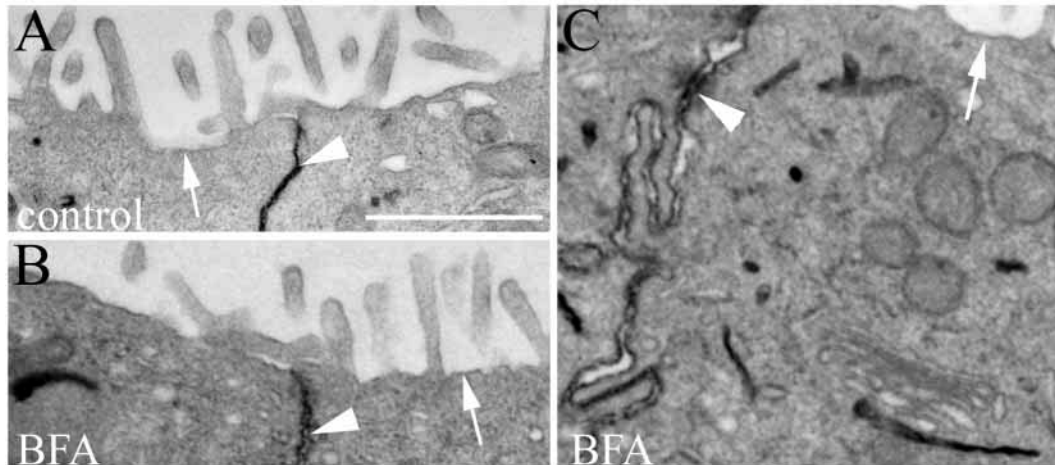


Fig. 2. Apical redistribution of TfR does not result from diffusion across disrupted tight junctions. Transmission electron micrographs are shown of control cells (A) and cells pretreated for 15 minutes with 10 μM BFA (B,C) and then incubated basolaterally with 15 $\mu\text{g}/\text{ml}$ HRP-Tf in the presence or absence of BFA for another 30 minutes. In all cases, the HRP reaction product is limited to endosomes and to the basolateral membrane (arrowheads), ending abruptly at the tight junction, with no product present at the apical plasma membrane (arrows). Scale bar, 1 μm (A,B); 0.5 μm (C).

cells were incubated with basolateral and apical Tf for 20 minutes, treated with BFA and the incubation continued. The initial incubation in probes results in strong labeling by basolateral Alexa568-Tf, but after as little as 8 minutes apical uptake of Alexa488-Tf is apparent, becoming more pronounced with time.

To ensure that uptake of apically applied Tf does not result from leakage of Alexa488-Tf to basolateral side of the cells, the effects of BFA on tight junction permeability were evaluated. Consistent with previous studies (Prydz et al., 1992), we find that the integrity of tight junctions is not affected by the drug treatments used in these studies, as reflected by the retention of 70 kDa dextran added to the basolateral side of an epithelial monolayer. Vertical sections of living monolayers of cells incubating in fluorescein dextran are shown in Fig. 1F-H. The fluorescent dextran is limited to the basolateral space for both untreated cells (Fig. 1F) and for cells following a 45 minute exposure to BFA (Fig. 1G). In contrast, fluorescent dextran is found to leak into the apical space when tight junctions are disrupted by incubating cells in Ca^{2+} -free PBS (Fig. 1H). In a parallel experiment, measurements of dextran fluorescence in the apical chamber demonstrated that dextran permeability of BFA-treated cells was indistinguishable from that of control cells, and tenfold less than that of cells incubated in calcium-free PBS (data not shown).

Apical uptake of Tf might also result from apical redistribution of TfR within the plane of the plasma membrane, if BFA disrupts the 'fence' function of the tight junctions. This possibility was evaluated by electron microscopy of cells incubated basolaterally with Tf conjugated to horseradish peroxidase (HRP-Tf). This conjugate is limited to the basolateral membrane and endosomes of both control cells (Fig. 2A) and cells treated with BFA (Fig. 2B). The labeling of the basolateral, but not apical membrane of BFA-treated cells is especially clear in Fig. 2C, which also shows several of the extended tubular endosomes characteristic of BFA-treated cells.

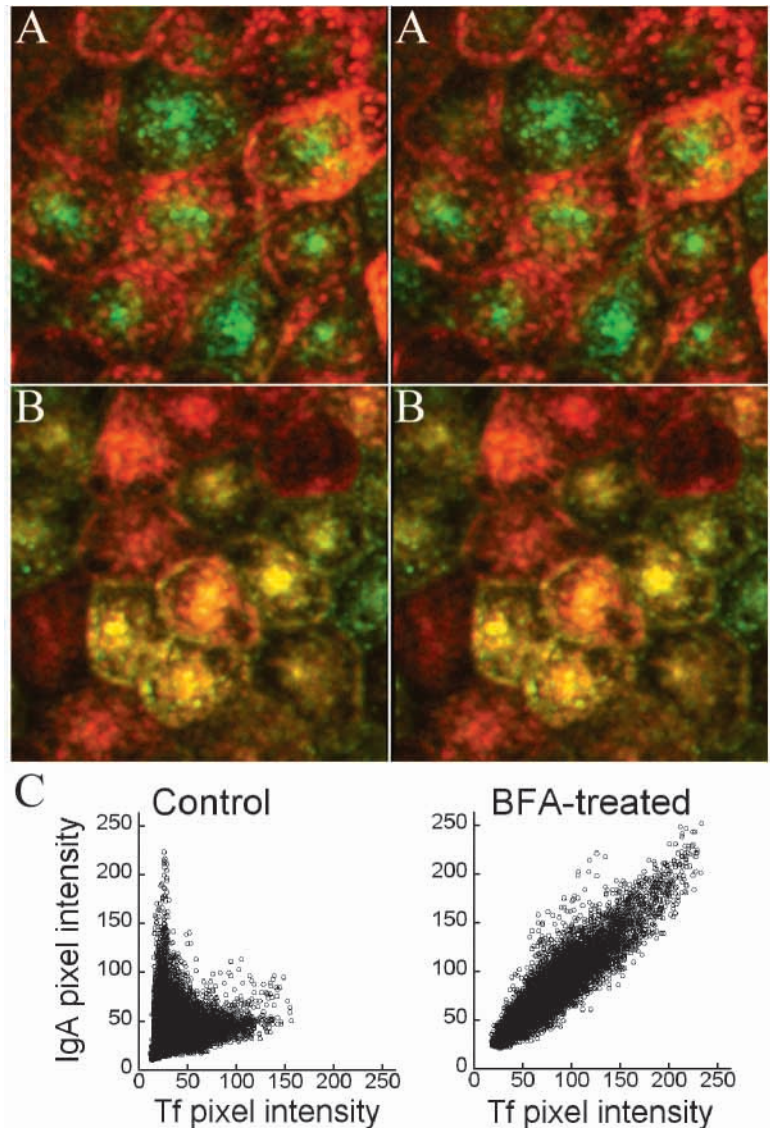
BFA blocks sorting of transcytosing IgA from recycling Tf

We have previously shown that Tf and IgA are both internalized into the same medial endosomes from which Tf is recycled, and IgA is directed to the ARE (Brown et al., 2000). In fact the efficiency with which IgA is sorted from Tf corresponds to the relative enrichment of IgA that occurs during transport from the common endosomes to the ARE, demonstrating that polar sorting occurs in common endosomes. The sorting of IgA from Tf is apparent in the field of living cells shown in the stereopair image of Fig. 3A. At steady state, Tf and IgA are both found in medial endosomes (appearing orange by combination), but the ARE is enriched in IgA alone (green). However, when cells are treated with BFA prior to uptake, no such sorting is apparent, and Tf and IgA are both delivered to apical endosomes (Fig. 3B). Indeed, the lack of sorting is apparent in the nearly constant color of the endosomes of each cell, reflecting a constant ratio of Tf to IgA in all the compartments in the cell.

The relative amounts of Tf and IgA in endosomes in living cells can be evaluated graphically, by plotting the red and green intensities of individual pixels from projected image volumes (see Materials and Methods). In order to pool data from cells expressing different relative numbers of pIgR and TfR, the pixel intensities are standardized such that the total red and green fluorescence is equivalent in each cell. The resulting plots can be used to distinguish endosomes according to their relative Tf and IgA fluorescence, similar to a flow cytometry analysis. Fig. 3C shows the results of analyzing 8 control or BFA-treated cells. Two classes of endosomes are found in control cells, one with a high ratio of Tf to IgA and a second with a very high ratio of IgA to Tf, correlating to medial endosomes and the ARE, respectively. These two populations of endosomes disappear in cells treated with BFA, replaced by a single population of endosomes with an intermediate ratio of Tf to IgA.

The effect of BFA on sorting of IgA from Tf was also addressed biochemically. The endocytic pathway of cells was

Fig. 3. BFA blocks intracellular sorting of Tf from IgA. 3-D images of living, polarized PTR cells were collected in the presence of basolateral Oregon Green-IgA and TxR-Tf after 30 minutes of uptake (A), and following 15 minutes of pretreatment in 10 μ M BFA and 35 minutes incubation with probes in the continued presence of BFA (B). In control cells, the sorting of IgA from Tf is apparent in the enrichment of IgA (green) in the ARE lacking Tf (red), whereas both IgA and Tf completely codistribute in BFA-treated cells, resulting in a nearly uniform endosome color in each cell. Each field is 40 μ m across. (C) Plots of individual pixel intensities from projected image volumes of control and BFA-treated cells, labeled and imaged as described above. Data represent the pooled data of 8 cells from each condition, with data normalized such that the mean IgA and Tf fluorescence are equal. Sorting of IgA is apparent in the enrichment of IgA in the ARE, represented by the population of pixels with a high ratio of IgA/Tf, relative to the common endosomes, whose pixels show a low ratio. In contrast, only a single population of pixels is found in cells treated with BFA.



preloaded with HRP-Tf by incubating cells in the presence of the ligand for 30 minutes and all subsequent incubations were done in the presence of HRP-Tf. Cells were then allowed to bind 125 I-Tf and 125 I-IgA on ice for 1 hour. Unbound radio-ligands were washed away, and cells were then incubated for 15 minutes in the absence or presence of 10 μ M BFA. After various intervals at 37°C, internalization of radio-ligands was stopped by placing the cells on ice. Cells were then treated with DAB and H₂O₂, and solubilized with detergent. In this assay, exposure to DAB and H₂O₂ mediates the HRP-catalyzed crosslinking of proteins present in endosomes containing HRP-Tf, so that sorting of IgA from Tf is evident in the increased amount of soluble 125 I-IgA. In Fig. 4A detergent soluble proteins were separated by SDS-PAGE. In control cells an increasing amount of 125 I-IgA is found in the detergent-soluble fraction with time, whereas in BFA-treated cells, relatively little 125 I-IgA is soluble throughout the timecourse. In a separate study, in which 125 I-Tf was omitted, the percentage of total cell-associated 125 I-IgA in the detergent-soluble fraction was quantified as a function of time for control cells or cells treated with BFA or the microtubule-depolymerizing reagent nocodazole (Fig. 4B). Whereas in both control and nocodazole-treated cells, IgA is increasingly found in the detergent-soluble fraction, reflecting sorting of IgA from HRP-Tf, a relatively small percentage of IgA escapes cross-linking in BFA-treated cells.

In order to confirm that sorting of ligand occurred in endosomes, we assayed pre-internalized ligands. Cells were incubated with 125 I-IgA and HRP-Tf for 5 minutes at 37°C, then transferred to ice, at which point surface ligands were stripped with an acid wash. Cells were then either kept on ice, or incubated at 37°C for 15 minutes, in the presence or absence of BFA. Samples were then processed as described above to cross-link HRP-Tf-containing endosomes. Fig. 4C shows that, similar to the results shown in Fig. 4B, after 15 minutes of incubation approximately 50% of pre-internalized IgA is sorted from HRP-Tf containing compartments in control cells,

whereas less than 25% is sorted from HRP-Tf in cells treated with BFA. As in the study shown in Fig. 4B, approximately 90% of the internalized IgA is initially contained in endosomes containing HRP-Tf, demonstrating that the two are internalized into the same compartment and are subsequently sorted from one another. The specificity of crosslinking is indicated by the fact that less than 10% of internalized IgA is found in the detergent-insoluble pellet when H₂O₂ is omitted.

The compartments of the transcytotic pathway are distinct in BFA-treated cells

If BFA induces apical transport of Tf by blocking sorting of Tf from IgA, it might be expected to induce transport of Tf to the ARE. In Fig. 3B, it is clear that BFA induces transport of Tf to condensed apical compartments, suggesting that BFA induces missorting of Tf to the ARE, from which it is normally excluded.

However, previous studies have demonstrated that BFA induces fusion and tubulation of endosomes (Hunziker et al., 1991; Lippincott-Schwartz et al., 1991; Wood et al., 1991; Wagner et al., 1994). Similarly, we find that BFA alters the

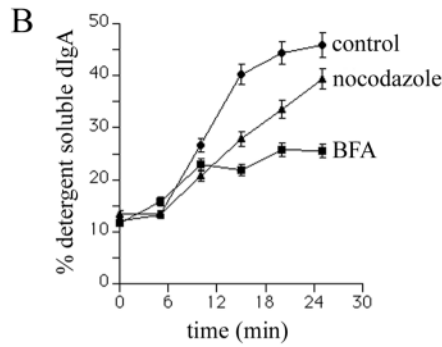
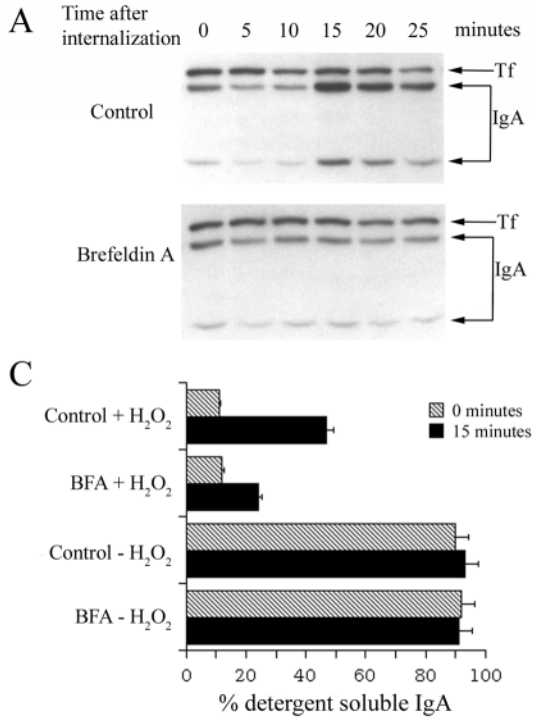


Fig. 4. BFA blocks intracellular sorting of Tf from IgA. This biochemical sorting assay is fully described in the Materials and Methods. Briefly, cells were incubated basolaterally with HRP-Tf for 30 minutes at 37°C, then placed on ice and incubated with HRP-Tf, ¹²⁵I-IgA and ¹²⁵I-Tfn for 60 minutes. Excess ligand was rinsed away, and cells were incubated in HRP-Tf in the absence or presence of 10 μM BFA for 15 minutes, and then

warmed to 37°C. At the indicated times cells were treated with DAB and H₂O₂ and solubilized. (A) SDS-PAGE and autoradiography of ¹²⁵I-Tf and ¹²⁵I-IgA present in the detergent-soluble fraction following internalization of ligands for the indicated periods of time in the absence or presence of 10 μM BFA. (B) The percentage of pre-bound ¹²⁵I-IgA in the detergent-soluble fraction is plotted as a function of time of internalization for control cells (circles), BFA-treated cells (squares) and cells treated with 33 μM nocodazole (triangles). (C) BFA blocks sorting of pre-internalized IgA and Tf. ¹²⁵I-IgA and HRP-Tf were internalized for 5 minutes at 37°C, then non-internalized ¹²⁵I-IgA was removed by acid wash on ice. BFA was then added for 15 minutes (with the cells still on ice) and the cells then either kept on ice (0 minutes) or incubated at 37°C for 15 minutes and analyzed.

morphology of endosomes of MDCK cells. In Fig. 5A, an image volume of living MDCK cells expressing GFP-Rab25, a protein associated with the transcytotic pathway of epithelial cells (Casanova et al., 1999), shows that Rab25 is normally found in punctate endosomes throughout the cell. However, upon treatment with BFA, endosomes become enlarged and elongated along the entire height of the cells, appearing interconnected (Fig. 5B). It is possible that, rather than inducing missorting of Tf from the common endosomes to the distinct ARE, BFA induces fusion of the sequential compartments of the transcytotic pathway. Accordingly, altered polar transport of both Tf and IgA may reflect the relatively non-specific consequence of generally impaired transport from an aberrant compartment.

In order to test whether the sequential compartments of the transcytotic pathway are distinct in cells treated with BFA, we evaluated the pH of endosomes in BFA-treated cells using ligands conjugated to both fluorescein and rhodamine. We previously demonstrated that the ARE could be distinguished from the common endosomes preceding it by a sharply higher pH (Wang et al., 2000). Tf, which is normally excluded from the ARE, is restricted to uniformly acidic medial endosomes in control cells, which appear orange due to the quenching of fluorescein (Fig. 6A). However, in cells treated with BFA, Tf is found not only in medial, acidic endosomes, but also in relatively alkaline apical compartments, which appear green due to the bright fluorescein fluorescence at higher pH (Fig. 6B).

Fig. 7A,B,E,F shows a field of living cells

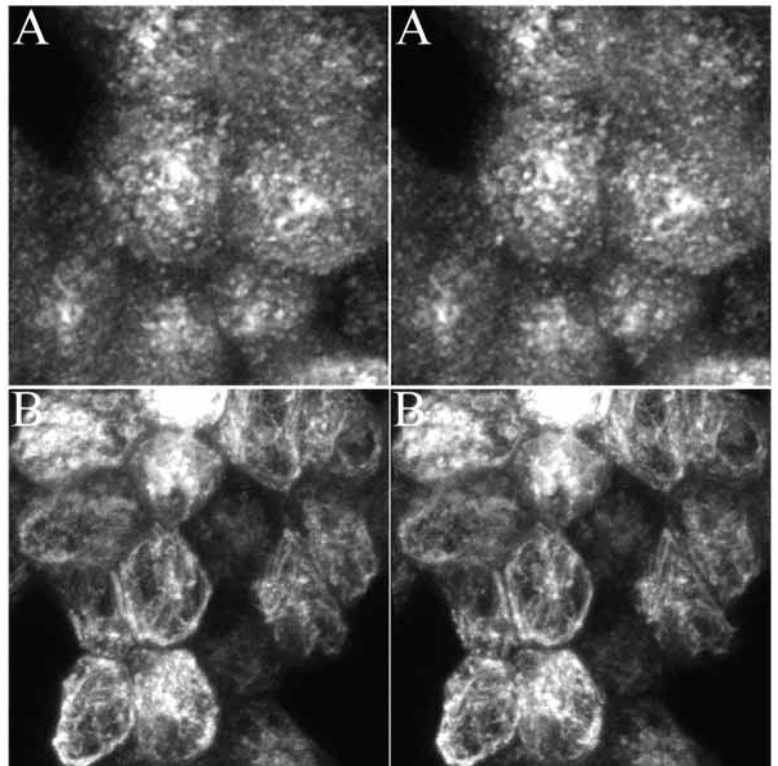
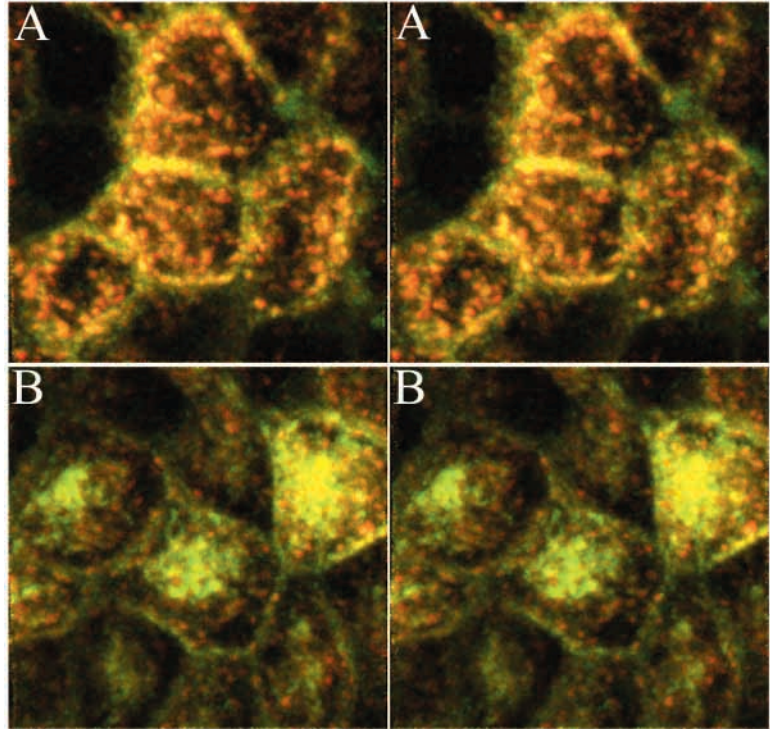


Fig. 5. BFA induces tubulation of endosomes associated with GFP-Rab25. 3-D stereopair images of living, polarized MDCK cells stably expressing GFP-Rab25 were collected for untreated cells (A) and cells following 40 minutes incubation in BFA (B). In untreated cells GFP-Rab25 labels punctate compartments, particularly at cell apices, whereas in cells treated with BFA, GFP-Rab25 is found on tubular compartments that extend vertically throughout the cells. Panel A is 24 μm in height, Panel B is 36 μm in height.

Fig. 6. Endosomes of the transcytotic pathway remain distinct in BFA-treated cells. 3-D stereopair images of living, polarized PTR cells were collected in the presence of basolateral Tf conjugated to both fluorescein and rhodamine (FR-Tf). The pH-sensitive fluorescence of fluorescein gives this probe a green fluorescence in the neutral environment of probe bound to the plasma membrane (note bases of cells in A), but an orange fluorescence for Tf in acidic endosomes. Whereas Tf is restricted to acidic endosomes in control cells (A), it is found in both acidic medial endosomes and relatively alkaline apical compartments in cells previously incubated with BFA for 15 minutes, and then in BFA with FR-Tf for another 22 minutes (B). Panels A and B are 34 μm in height.



incubating with both pH-sensitive FR-Tf and Cy5-IgA. Images collected at the apex of the cells show that Tf is excluded from the condensed ARE in which IgA accumulates (Fig. 7A,B). Images collected in a medial plane (Fig. 7E,F) show that Tf closely colocalizes with IgA in acidic (orange) medial endosomes of the same cells. In contrast, after BFA treatment, Tf codistributes with IgA throughout the cell, in both acidic medial endosomes and in relatively alkaline apical compartments. The apical plane of BFA-treated cells shown in Fig. 7C,D shows that Tf colocalizes with IgA in alkaline apical compartments, which appear yellow to green in color.

A medial focal plane from another field of cells is shown in Fig. 7G,H, in which Tf and IgA are found to colocalize in orange, acidic endosomes, as well as in a distinctly alkaline tubule at the top of the field. The sharply higher pH of the apical compartments suggests that the ARE remains distinct in cells treated with BFA. The same distinction is apparent in cells labeled with FR-IgA. Similar to our previous studies (Wang et al., 2000), IgA is normally found in both acidic endosomes and in relatively alkaline AREs, as shown in the apical focal plane shown in Fig. 7I where the acidic endosomes surround the central ARE. These two compartments remain distinct in cells treated with BFA (Fig. 7J,K). Due to variations in cell height, the single optical section shown in Fig. 7J images acidic medial endosomes of some cells (the center 3), and alkaline apical AREs of others (top and bottom). Fig. 7K is an image showing more of the alkaline AREs. These results indicate not only that the AREs are distinct from the common endosomes of BFA-treated cells, but also that BFA induces missorting and transport of Tf from the common endosome to the ARE.

Studies of cells labeled with Tf and LDL indicate that the effects of BFA are limited to sorting in the common endosome. We previously found that sorting of Tf from LDL occurs in a separate step that precedes polar sorting of Tf from IgA (Brown et al., 2000). This sorting is apparently intact in cells treated with BFA, as Tf is found distributed largely in tubular compartments and LDL is restricted to punctate compartments, some of which also contain Tf, some of which contain LDL alone (Fig. 7L). The transport of Tf into tubular compartments lacking LDL demonstrates that Tf is sorted from LDL in BFA-treated cells. This observation suggests that the effect of BFA is specific to polar sorting in the common endosome, and also demonstrates that sorting endosomes (containing both Tf and LDL) are distinct from (although perhaps physically

continuous with) the common endosomes containing Tf and IgA.

Taken together, these studies demonstrate that apical missorting of TfR does not derive from gross fusion of endocytic compartments. The fact that transport through distinct sorting endosomes, common endosomes and AREs continues in the presence of BFA allows us to delimit the effects of BFA to polar sorting in the common endosome, where it blocks exclusion of TfR from the transcytotic pathway.

BFA induces transport of Tf to compartments associated with Rab11a and Rab25

The pH and location of the apical compartment of BFA-treated cells suggests that BFA induces transport of Tf to the ARE. The identification of this compartment as the ARE is supported by our observations of living cells expressing GFP chimeras of Rab25 and Rab11a, two markers of the ARE (Casanova et al., 1999). Images of living cells stably expressing GFP-Rab25 are presented in Fig. 8A-F. In control cells, Rab25 prominently associates with the ARE, the extreme apical compartment in which basolateral IgA accumulates (Fig. 8A,B). Consistent with previous studies showing that Tf is excluded from the ARE (Brown et al., 2000; Wang et al., 2000), the apical compartment containing the vast majority of GFP-Rab25 lacks Tf, with the bright GFP-Rab25 fluorescence corresponding to gaps in the fluorescence pattern of Tf (Fig. 8C,D). Fig. 8E,F shows that upon treatment with BFA, the apical GFP-Rab25 compartment remains apparent, but is now accessible to basolaterally internalized Tf.

Similar observations are made in living cells transiently expressing GFP-Rab11a (Fig. 8G-L). As with Rab25, GFP-Rab11a prominently associates with the apical compartment in which IgA accumulates (Fig. 8G,H), but which lacks Tf (Fig.

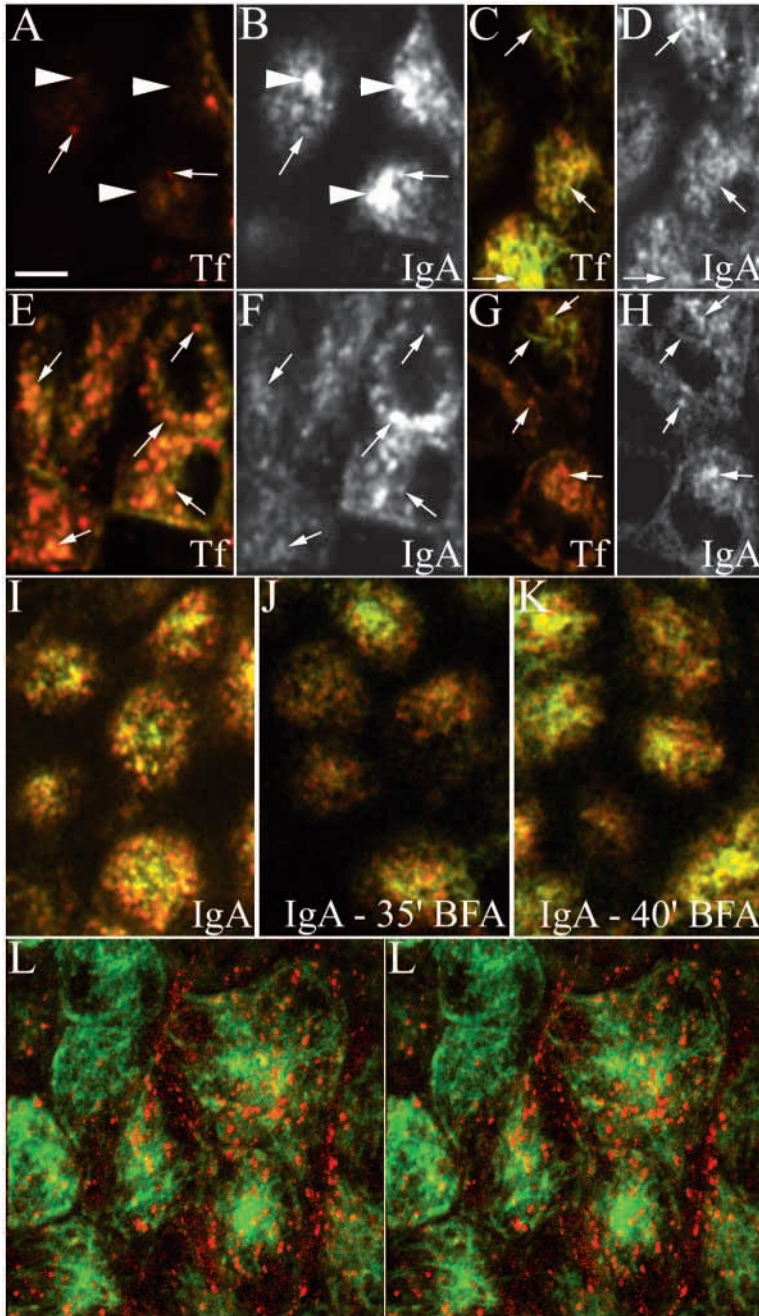


Fig. 7. BFA induces transport of both Tf and IgA to the same alkaline apical endosomes. (A-H) Cells were labeled to steady state and imaged alive in the presence of FR-Tf and Cy5-IgA. An apical optical section of control cells shows that FR-Tf (A) is missing from the AREs in which Cy5-IgA concentrates (arrowheads in A,B). In a lower focal plane of the same cells, the two probes closely colocalize in uniformly acidic endosomes (arrows in E and F). In cells treated with BFA for 15 minutes, and then incubated for 25 minutes in probes and BFA, FR-Tf is delivered to apical, alkaline compartments containing Cy5-IgA (arrows in C and D). A separate field of cells, incubated for 15 minutes with BFA, then with probes and BFA for 45 minutes (G,H) shows the two are closely colocal in medial acidic (orange) compartments as well as in alkaline tubular endosomes (green, at the top of the panel). (I) A field of untreated cells imaged in the presence of FR-IgA shows that IgA is located in both acidic endosomes as well as in relatively alkaline AREs located at the cell apices. These two distinct compartments are apparent also in images of cells incubated with BFA for 15 minutes, then with BFA and FR-IgA for another 20 (J) or 25 (K) minutes, showing IgA present in both medial acidic endosomes and relatively alkaline apical endosomes. Note that because of differences in cell height, single optical sections collect apical planes of some cells and medial planes of others. (L) Sorting endosomes remain distinct after protracted exposure of cells to BFA. 3-D images of living, polarized PTR cells were collected in the presence of basolateral Alexa488-Tf and diI-LDL following a 15 minute pretreatment with BFA and an 85 minute incubation with both BFA and fluorescent ligands. Whereas Tf is largely distributed into extended tubules, LDL, found in both sorting endosomes containing Tf and in late endosomes lacking Tf, is restricted to vesicular compartments. Panel L is 29 μm in height.

8I,J). After treatment with BFA, Tf and GFP-Rab11a are broadly colocalized, and in particular, Tf is found in the extreme apical compartment associated with Rab11a (Fig. 8K,L).

Taken together, these results suggest that BFA induces transport of Tf to the ARE, as identified by its apical location, relatively alkaline pH, and association with Rabs 11a and 25.

BFA-sensitive association of γ -adaptin with endosomes containing IgA

Brefeldin A alters membrane transport by blocking the association of ADP ribosylation factor (ARF) with membranes, in turn dissociating ARF-dependent coatamers, such as β -COP and γ -adaptin from membranes (Donaldson et al., 1992).

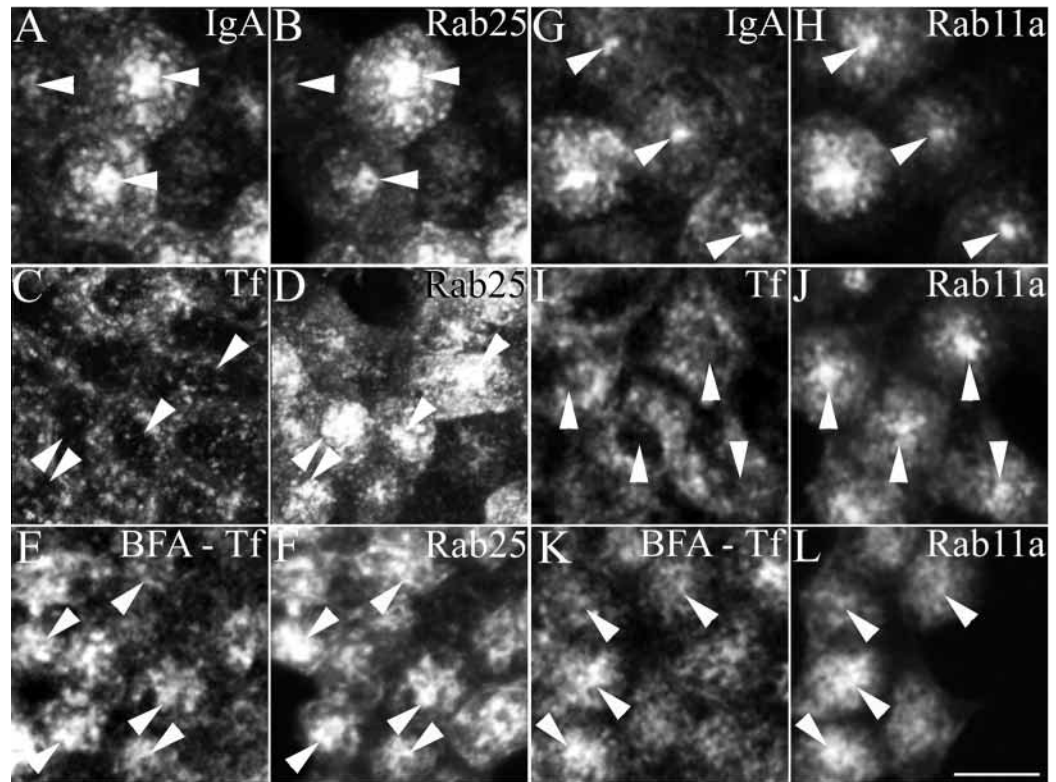
Ultrastructural analysis of MDCK cells revealed that γ -adaptin, generally associated with Golgi transport, is associated with endosomal buds from which recycling vesicles form (Futter et al., 1998). Based upon the observation that BFA both dissociated γ -adaptin from endosomes, and also increased apical Tf transport, Futter et al. suggested that BFA increases apical Tf transport by blocking membrane association of γ -adaptin, which in turn blocks sequestration of Tf into recycling vesicles (Futter et al., 1998).

In control cells, γ -adaptin was immunolocalized to both punctate and large tubular compartments (Fig. 9A). The tubular compartments are likely to correspond to the TGN as they lacked the endocytic probes Tf or IgA (data not shown). Treatment of cells with BFA both dissociated the majority of γ -adaptin from intracellular compartments and simultaneously produced extended tubular endosomes in cells incubated with Tf (Fig. 9B,C).

In control cells, the distributions of Tf and γ -adaptin showed little vesicle-for-vesicle agreement (Fig. 9D-F). In contrast, the distribution of γ -adaptin closely resembled that of IgA. The correspondence was especially close in the ARE imaged in apical planes (Fig. 9G-I), but in medial planes of the same cells, individual vesicles could be identified that both included IgA and associated with γ -adaptin (Fig. 9J-L).

These images suggest that γ -adaptin is more closely associated with transcytotic compartments (containing IgA) than with recycling compartments (containing Tf), suggesting

Fig. 8. BFA induces transport of Tf to apical endosomes associated with Rab25 and Rab11a. (A,B) Image volumes of living cells stably expressing GFP-Rab25 incubated to steady state with basolateral Alexa568-IgA were collected, and reproduced as extended focus projections. IgA and Rab25 closely colocalize, in particular Rab25 is strongly associated with the ARE in which IgA accumulates (arrowheads). (C,D) Image volumes collected of living cells incubated with Alexa568-Tf show that Tf is absent from AREs, so that the apical GFP-Rab25 concentrations correlate with holes in the projected Tf images (arrowheads). (E,F) Images of an apical plane of cells pretreated with BFA for 20 minutes, then incubated with Alexa568-Tf in the continued presence of BFA for another 30 minutes show that BFA induces redirection of Tf



into the apical compartments associated with GFP-Rab25. (G,H) Extended focus images of living cells expressing GFP-Rab11a show that, similar to Rab25, Rab11a closely codistributes with basolaterally internalized Alexa568-IgA, particularly in AREs, which again appear as holes in extended focus images of Tf (I,J). (K,L) An apical plane of GFP-Rab11a-expressing cells pretreated with BFA for 20 minutes, then incubated with Alexa568-Tf in the continued presence of BFA for another 30 minutes shows that BFA induces redirection of Tf to the apical compartments associated with GFP-Rab11a. Scale bar, 15 μm (A,B); 10 μm for the remaining panels.

that γ -adaptin plays a role in transcytotic transport. This subjective impression is supported by a quantitative analysis of the correlation between the 3-D distribution of γ -adaptin and Tf or IgA. For these studies, cells were labeled with either Tf or IgA, then processed for γ -adaptin immunofluorescence. 3-D image volumes were then collected for both the endocytic ligands and γ -adaptin. As explained in Materials and Methods, the cytoplasmic volumes of individual cells were then outlined, and correlation coefficients calculated for the comparison of γ -adaptin with either Tf or IgA.

As might be expected for a protein largely associated with the biosynthetic pathway, the distribution of γ -adaptin does not correlate highly with either that of Tf or IgA. However, the correlation between γ -adaptin and IgA is roughly twice that between γ -adaptin and Tf (0.29 ± 0.05 versus 0.14 ± 0.04 , $P < 0.0001$, Student's *t*-test) (Fig. 10A). These data are summarized in Fig. 10B, which also presents data demonstrating the appropriate behavior of the analysis. Correlation coefficients for cells labeled basolaterally with a combination of Alexa488-Tf and Alexa568-Tf (which would ideally show a perfect correlation) averaged 0.75 ± 0.04 . When one image volume of each of these pairs was rotated 180° (thus producing uncorrelated distributions), the mean correlation between image volumes dropped to 0.01 ± 0.07 .

These results indicate that γ -adaptin is more closely associated with the endocytic pathway followed by IgA than that followed by Tf. The fact that, similar to previous studies

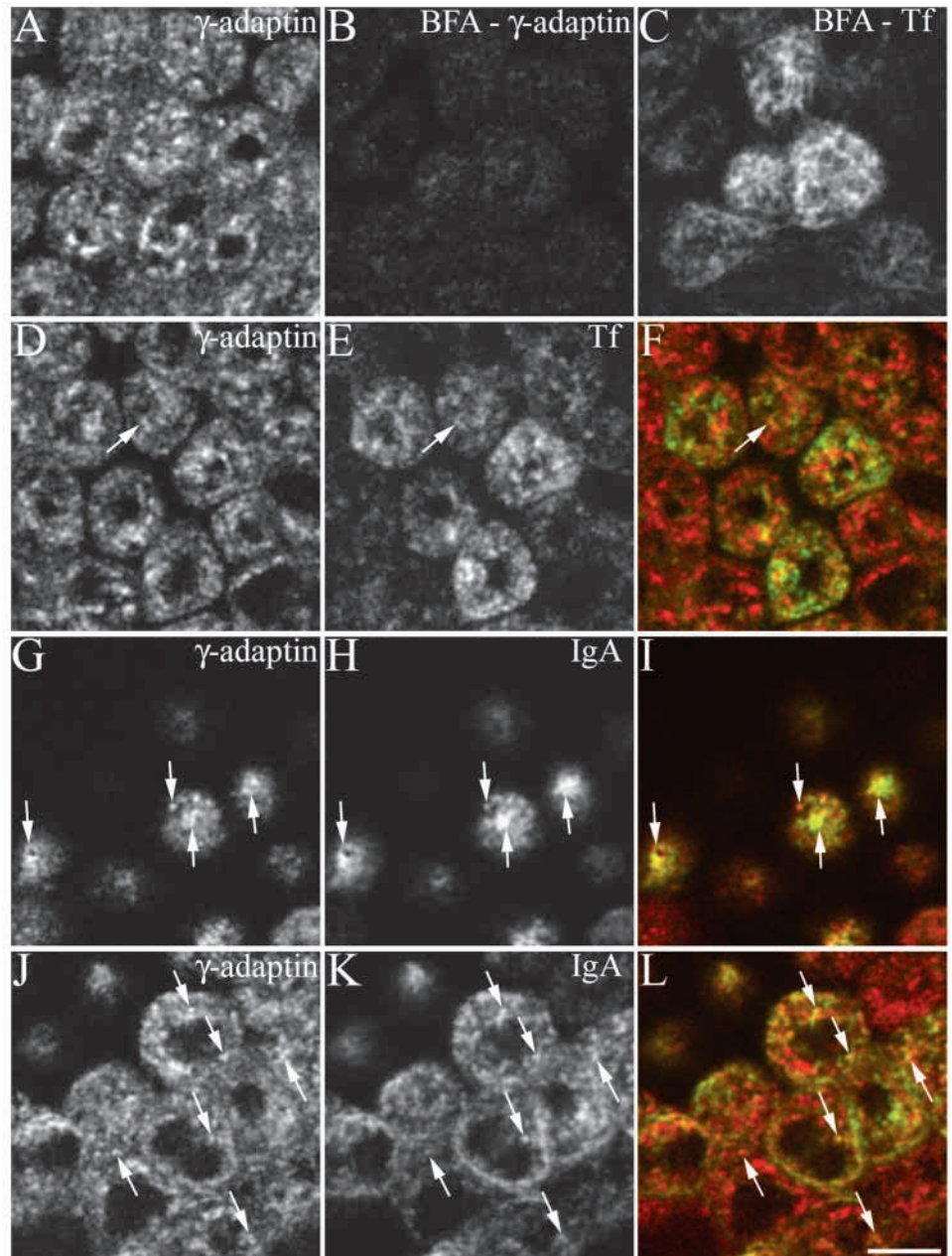
(Okamoto et al., 1998), γ -adaptin was found to associate with the ARE indicates that γ -adaptin is unlikely to be specifically involved in basolateral recycling.

DISCUSSION

While BFA has generally been observed to modestly affect endocytic membrane transport in fibroblasts, BFA profoundly alters the endocytic pathways of polarized MDCK cells. In various studies BFA has been observed to stimulate apical transport and slow basolateral recycling of TfR (Wan et al., 1992; Matter et al., 1993; Futter et al., 1998), to inhibit apical transcytosis, without affecting basolateral recycling of IgA (Hunziker et al., 1991; Barroso and Sztul, 1994), to selectively stimulate apical endocytosis and to stimulate basolateral to apical transcytosis of fluid markers (Prydz et al., 1992). On the basis of observations that BFA induced transcytosis of chimeric LDL receptors with basolateral sorting determinants, but stimulated transcytosis of chimeras lacking basolateral determinants, Matter et al. (Matter et al., 1993) suggested that BFA interfered with polar sorting, rather than with any particular transport pathway. Recent studies suggested that BFA might disrupt polar sorting by interfering with the formation of recycling endosomes in which basolateral proteins are concentrated (Futter et al., 1998).

However, BFA has also been found to disrupt the

Fig. 9. γ -adaptin is associated with IgA-containing endosomes. (A) In a medial plane of polarized cells, immunolocalized γ -adaptin associates with multiple intracellular compartments. Punctate compartments correspond to endosomes (see below) while larger tubular structures are likely to be elements of the trans-Golgi network. Treatment of cells with BFA both dissociates γ -adaptin from intracellular compartments, and also tubulates endosomes, as shown in the medial plane of a field of cells pretreated with BFA for 15 minutes, then incubated with Alexa488-Tf for 40 minutes in the continued presence of BFA (B,C). A medial plane of control cells incubated with Alexa488-Tf shows a limited colocalization of Tf with γ -adaptin (D-F). In contrast, cells incubated with Alexa488-IgA show a close correspondence between the distributions of IgA and γ -adaptin. This colocalization is particularly apparent in apical planes, where the patterns of the two closely match in AREs and punctate endosomes (G-I), but also in the focal plane of the same cells collected 6 microns lower (J-L), where the two colocalize in medial endosomes. A few examples of IgA-containing endosomes associated with γ -adaptin are noted with arrows. Scale bar, 10 μ m.



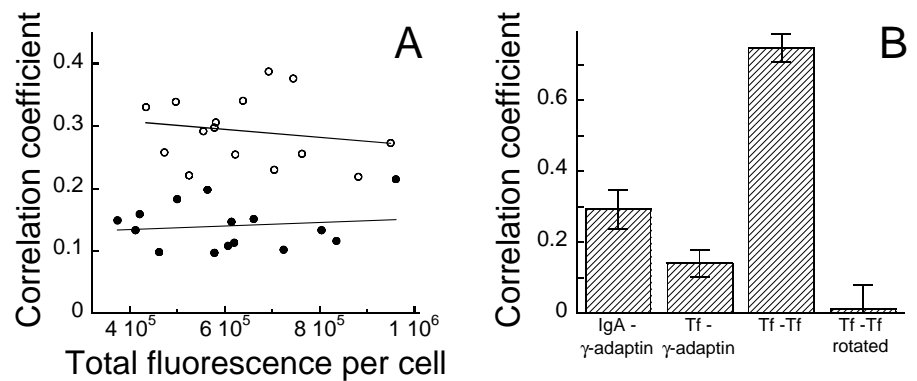
morphology of endosomes, causing extensive tubulation and fusion of early endosomes and the TGN (Lippincott-Schwartz et al., 1991; Wood et al., 1991; Tooze and Hollinshead, 1992; Wagner et al., 1994; Stoorvogel et al., 1996). Gross disruption of endocytic compartments, and particularly fusion of sequential endocytic compartments could also explain the generally disrupted, ectopic protein targeting described in the studies listed above. In order to address the effects of BFA on endocytic sorting of TfR and IgA, we used microscopy of living cells to evaluate how defined endocytic compartments are affected by BFA and to characterize the intracellular transport of Tf and IgA through these compartments.

We previously characterized the endocytic itineraries of MDCK cells (Brown et al., 2000). After internalization into the same basolateral sorting endosomes, IgA and Tf are sorted from lysosomally destined LDL and directed to common

endosomes. While Tf is directly recycled to the basolateral membrane, IgA is transcytosed to the ARE and then to the apical plasma membrane.

The analyses of living MDCK cells presented here show that the sequential compartments of the transcytotic pathway remain distinct from one another in the presence of BFA. Common endosomes (identified as containing Tf and IgA, but not LDL) form extensive tubules distinct from sorting endosomes (identified as containing both Tf and LDL), which are refractory to tubulation, remaining punctate in the presence of BFA. The ARE, which also tubulates in BFA, remains distinct from common endosomes, as judged by its sharply higher pH, and its extreme apical location, similar to untreated cells. These results indicate that the effects of BFA on membrane transport in MDCK cells do not reflect gross fusion of endocytic compartments.

Fig. 10. Correlation analysis shows γ -adaptin is more closely associated with endosomes containing IgA than with those containing Tf. Correlation coefficients were calculated comparing the 3-D distributions of γ -adaptin and either Tf or IgA (see Materials and Methods). Briefly, cells were labeled to steady state with either Tf or IgA, and then processed for γ -adaptin immunofluorescence. 3-D image volumes were collected, and 15 cells from each condition selected for correlation analysis. (A) Correlation coefficients, calculated for individual cells, are plotted against the total fluorescence of internalized Tf (closed circles) or IgA (open circles). Although variable, the correlations between IgA and γ -adaptin were uniformly higher than those between Tf and γ -adaptin, and largely independent of the levels of Tf or IgA fluorescence. (B) Bar graphs of the pooled data show a mean correlation coefficient of 0.29 ± 0.05 between IgA and γ -adaptin, and a mean correlation coefficient of 0.14 ± 0.04 between Tf and γ -adaptin. The potential range of this assay is demonstrated in cells labeled with a combination of Alexa488-Tf and Alexa568-Tf, which codistribute in the same compartments. Analysis of 15 cells yielded a mean correlation of 0.75 ± 0.04 . The mean correlation coefficient dropped to 0.01 ± 0.07 when the region of analysis of one image of each pair was rotated 180° .



Transport along the transcytotic pathway is likewise intact in cells treated with BFA, but is now visited by Tf as well as IgA, with the result that the basolateral polarity of TfR is lost within minutes of addition. As with control cells, in the presence of BFA Tf is found in both punctate sorting endosomes containing LDL, as well as in medial, tubular, acidic compartments containing IgA, but not LDL. In contrast to control cells, however, Tf is also transported to AREs, as identified by their extreme apical location, nearly neutral pH and association with Rabs 11a and 25. Thus BFA blocks polar sorting of Tf away from the transcytotic pathway. The specificity of this effect is indicated by the observation that sorting in sorting endosomes is intact in cells treated with BFA. Tf and IgA are sorted from punctate sorting endosomes containing LDL into tubules lacking LDL, and LDL is sorted into compartments lacking either Tf or IgA. Thus while polar sorting in common endosomes is sensitive, lysosomal sorting in sorting endosomes continues in BFA. This observation is consistent with previous studies showing Fc receptor-mediated degradation of IgG complexes is unaffected by BFA (Hunziker et al., 1991).

BFA is believed to alter membrane transport by inhibiting the association of vesicle coat proteins, thus blocking the formation of transport vesicles. The effects of BFA on membrane transport in MDCK cells appear to be contradictory; whereas studies with Tf would indicate that recycling is inhibited and transcytosis is intact, studies of IgA indicate that transcytosis is inhibited with no effect on recycling. However, our results showing that BFA affects the segregation of recycling and transcytotic receptors without altering the overall integrity of the endocytic pathway indicate a significant transport of membrane in the absence of coats. Endosomal coat proteins may play a more important role in sorting receptors into different pathways, either by clustering them at vesicle budding sites or by excluding them from vesicles, rather than in vesicle formation per se. Our data is consistent with a model in which BFA-sensitive coat proteins are required for efficient sorting into the recycling and transcytotic pathways. Thus, in the absence of coats and sorting, the different receptors may distribute along both pathways, perhaps reflecting bulk

membrane flow (e.g. non-coat concentrated transport). In the case of Tf, this would result in an observed decrease in recycling coupled with an increase in transcytosis, while transcytosis of dIgA would be decreased with a concomitant intracellular accumulation and increase in recycling.

Our finding that BFA increases the direction of Tf to the ARE suggests that polar sorting of TfR is mediated by BFA-sensitive coats. It has recently been demonstrated that one such coat complex, a novel AP-1 adaptor complex, mediates basolateral sorting in epithelial cells. μ 1b, an epithelial-specific AP-1 medium chain that assembles with γ , β 1 and σ 1 into AP-1B adaptor complexes, has been found to both bind the polarity determinants in the cytoplasmic tail of TfR, and to mediate basolateral localization of TfR in epithelial cells (Folsch et al., 1999; Ohno et al., 1999). However, it is not known if AP-1B localizes to endosomes, nor if it mediates basolateral sorting of TfR at the level of endosomes, the TGN or both. Interestingly, AP-4, another BFA sensitive adaptor complex present on endosomes in MDCK cells is also involved in basolateral sorting (T. Simmen et al., unpublished).

Futter et al. (Futter et al., 1998) presented a model in which γ -adaptin, a component of AP-1 complexes, participates in forming coats that mediate diversion of basolateral membrane proteins into basolateral recycling vesicles. While our studies are generally consistent with this model, they demonstrate that γ -adaptin does not play a specific role in basolateral recycling. To the degree that γ -adaptin mediates basolateral recycling, it should closely associate with endosomes containing Tf. However, comparison of the distributions of Tf and γ -adaptin show a relatively poor correlation between the two. While Futter et al. (Futter et al., 1998) interpreted differences in distribution as reflecting γ -adaptin capping endosomes containing Tf, our studies indicate that the differences reflect the association of γ -adaptin with the transcytotic pathway. Quantitative analyses of fluorescence images demonstrate that γ -adaptin associates more closely with IgA than with Tf, indeed clearly associating with the ARE, a post-sorting transcytotic compartment. This observation is consistent with previous studies in which γ -adaptin was localized to the ARE of gastric epithelia (Okamoto et al., 1998), and with studies

indicating that AP-1 may bind to pIgR during transcytosis (Orzech et al., 1999).

The fact that γ -adaptin is more closely associated with the transcytotic pathway indicates that, while BFA may disrupt basolateral sorting of TfR by dissociating AP-1 from endosomes, AP-1 does not play a specific role in polar sorting via its participation in the formation of basolateral recycling vesicles. The presence of γ -adaptin on both the recycling and transcytotic pathways may also explain observations that BFA not only slows basolateral recycling of Tf, but also impairs apical transport of IgA (Hunziker et al., 1991) and of mutant forms of the LDL receptor that are normally efficiently transcytosed (Matter et al., 1993). These results are difficult to reconcile with a model in which BFA alters formation of a single type of transport vesicle and, taken with our results, indicate that BFA separately affects basolateral sorting of TfR and the apical transport of IgA without disrupting the overall endocytic pathways. It will now be important to determine which adaptors are associated with sorting into the recycling and transcytotic pathways.

This work was supported by NIH grant DK51098 (K.W.D.), NIH grants DK48370 and DK43405 and a Veterans Administration Merit Award (J.R.G.) and a fellowship from the American Heart Assn., Indiana Affiliate (E.W.). We would like to thank Jennifer Navarre Griner for invaluable assistance in the cloning of the GFP-Rab25 cell line.

REFERENCES

- Apodaca, G., Katz, L. A. and Mostov, K. E. (1994). Receptor-mediated transcytosis of IgA in MDCK cells is via apical recycling endosomes. *J. Cell Biol.* **125**, 67-86.
- Barroso, M. and Sztul, E. S. (1994). Basolateral to apical transcytosis in polarized cells is indirect and involves BFA and trimeric G protein sensitive passage through the apical endosome. *J. Cell Biol.* **124**, 83-100.
- Bomsel, M., Prydz, K., Parton, R. G., Gruenberg, J. and Simons, K. (1989). Endocytosis in filter-grown Madin-Darby canine kidney cells. *J. Cell Biol.* **109**, 3243-3258.
- Breitfeld, P. P., Casanova, J. E., Harris, J. M., Simister, N. E. and Mostov, K. E. (1989). Expression and analysis of the polymeric immunoglobulin receptor in Madin-Darby canine kidney cells using retroviral vectors. [Review] [10 refs]. *Meth. Cell Biol.* **32**, 329-337.
- Brown, P. S., Wang, E., Aroeti, B., Chapin, S. J., Mostov, K. E. and W. Dunn, K. (2000). Definition of distinct compartments in polarized Madin-Darby canine kidney (MDCK) cells for membrane-volume sorting, polarized sorting and apical recycling. *Traffic* **1**, 124-140.
- Casanova, J. E., Wang, X., Kumar, R., Bhartur, S. G., Navarre, J., Woodrum, J. E., Altschuler, Y., Ray, G. S. and Goldenring, J. R. (1999). Association of Rab25 and Rab11a with the apical recycling system of polarized Madin-Darby canine kidney cells. *Mol. Bio. Cell* **10**, 47-61.
- Donaldson, J. G., Finazzi, D. and Klausner, R. D. (1992). Brefeldin A inhibits Golgi membrane-catalysed exchange of guanine nucleotide onto ARF protein. *Nature* **360**, 350-352.
- Folsch, H., Ohno, H., Bonifacino, J. S. and Mellman, I. (1999). A novel clathrin adaptor complex mediates basolateral targeting in polarized epithelial cells. *Cell* **99**, 189-198.
- Futter, C. E., Gibson, A., Allchin, E. H., Maxwell, S., Ruddock, L. J., Odorizzi, G., Domingo, D., Trowbridge, I. S. and Hopkins, C. R. (1998). In polarized MDCK cells basolateral vesicles arise from clathrin-gamma-adaptin-coated domains on endosomal tubules. *J. Cell Biol.* **141**, 611-624.
- Hunziker, W., Whitney, J. A. and Mellman, I. (1991). Selective inhibition of transcytosis by brefeldin A in MDCK cells. *Cell* **67**, 617-627.
- Hunziker, W. and Peters, P. J. (1998). Rab17 localizes to recycling endosomes and regulates receptor-mediated transcytosis in epithelial cells. *J. Biol. Chem.* **273**, 15734-15741.
- Lippincott-Schwartz, J., Yuan, L., Tipper, C., Amherdt, M., Orci, L. and Klausner, R. D. (1991). Brefeldin A's effects on endosomes, lysosomes, and the TGN suggest a general mechanism for regulating organelle structure and membrane traffic. *Cell* **67**, 601-616.
- Matter, K., Whitney, J. A., Yamamoto, E. M. and Mellman, I. (1993). Common signals control low density lipoprotein receptor sorting in endosomes and the Golgi complex of MDCK cells. *Cell* **74**, 1053-1064.
- Maxfield, F. R. and Dunn, K. W. (1990). Studies of endocytosis using image intensification fluorescence microscopy and digital image analysis. In *Optical Microscopy for Biology* (ed. B. Herman and K. Jacobsen), pp. 357-371. New York: Alan R. Liss.
- Odorizzi, G., Pearse, A., Domingo, D., Trowbridge, I. S. and Hopkins, C. R. (1996). Apical and basolateral endosomes of MDCK cells are interconnected and contain a polarized sorting mechanism. *J. Cell Biol.* **135**, 139-152.
- Ohno, H., Tomemori, T., Nakatsu, F., Okazaki, Y., Aguilar, R. C., Folsch, H., Mellman, I., Saito, T., Shirasawa, T. and Bonifacino, J. S. (1999). Mu1B, a novel adaptor medium chain expressed in polarized epithelial cells. *FEBS Lett.* **449**, 215-220.
- Okamoto, C. T., Karam, S. M., Jeng, Y. Y., Forte, J. G. and Goldenring, J. R. (1998). Identification of clathrin and clathrin adaptors on tubulovesicles of gastric acid secretory (oxyntic) cells. *Am. J. Physiol.* **274**, C1017-C1029.
- Orzech, E., Schlessinger, K., Weiss, A., Okamoto, C. T. and Aroeti, B. (1999). Interactions of the AP-1 Golgi adaptor with the polymeric immunoglobulin receptor and their possible role in mediating brefeldin A-sensitive basolateral targeting from the trans-Golgi network. *J. Biol. Chem.* **274**, 2201-2215.
- Parton, R. G., Prydz, K., Bomsel, M., Simons, K. and Griffiths, G. (1989). Meeting of the apical and basolateral endocytic pathways of the Madin-Darby canine kidney cell in late endosomes. *J. Cell Biol.* **109**, 3259-3272.
- Pitas, R. E., Innerarity, T. L., Weinstein, J. N. and Mahley, R. W. (1981). Acetoacetylated lipoproteins used to distinguish fibroblasts from macrophages in vitro by fluorescence microscopy. *Arteriosclerosis* **1**, 177-185.
- Podbilewicz, B. and Mellman, I. (1990). ATP and cytosol requirements for transferrin recycling in intact and disrupted MDCK cells. *EMBO J.* **9**, 3477-3487.
- Prydz, K., Hansen, S. H., Sandvig, K. and van Deurs, B. (1992). Effects of brefeldin A on endocytosis, transcytosis and transport to the Golgi complex in polarized MDCK cells. *J. Cell Biol.* **119**, 259-272.
- Stoorvogel, W., Oorschot, V. and Geuze, H. J. (1996). A novel class of clathrin-coated vesicles budding from endosomes. *J. Cell Biol.* **132**, 21-33.
- Tooze, J. and Hollinshead, M. (1992). In AtT20 and HeLa cells brefeldin A induces the fusion of tubular endosomes and changes their distribution and some of their endocytic properties. *J. Cell Biol.* **118**, 813-830.
- van Steensel, B., van Binnendijk, E. P., Hornsby, C. D., van der Voort, H. T., Krozowski, Z. S., de Kloet, E. R. and van Driel, R. (1996). Partial colocalization of glucocorticoid and mineralocorticoid receptors in discrete compartments in nuclei of rat hippocampus neurons. *J. Cell Sci.* **109**, 787-792.
- Wagner, M., Rajasekaran, A. K., Hanzel, D. K., Mayor, S. and Rodriguez-Boulan, E. (1994). Brefeldin A causes structural and functional alterations of the trans-Golgi network of MDCK cells. *J. Cell Sci.* **107**, 933-943.
- Wan, J., Taub, M. E., Shah, D. and Shen, W. C. (1992). Brefeldin A enhances receptor-mediated transcytosis of transferrin in filter-grown Madin-Darby canine kidney cells. *J. Biol. Chem.* **267**, 13446-13450.
- Wang, E., Brown, P. S., Aroeti, B., Chapin, S. J., Mostov, K. E. and Dunn, K. W. (2000). Apical and basolateral endocytic pathways of MDCK cells meet in acidic common endosomes distinct from a nearly-neutral apical recycling endosome. *Traffic* **1**, 480-493.
- Wood, S. A., Park, J. E. and Brown, W. J. (1991). Brefeldin A causes a microtubule-mediated fusion of the trans-Golgi network and early endosomes. *Cell* **67**, 591-600.
- Yamashiro, D. J., Tycko, B., Fluss, S. R. and Maxfield, F. R. (1984). Segregation of transferrin to a mildly acidic (pH 6.5) para-Golgi compartment in the recycling pathway. *Cell* **37**, 789-800.